Ultrafast nonlinear optical responses and geometrical relaxations in π-conjugated polymers

Takayoshi Kobayashi

Department of Physics, University of Tokyo,
Hongo 7-3-1, Bunkyo-ku, Tokyo 113, Japan

ABSTRACT

In the present paper the following subjects are discussed about conjugated polymers: the first is a model of the relaxation of excitons, the second is the Raman spectrum of the excitons with 1ps lifetime, and the third is the optical Stark effect of the Raman gain spectrum.

(1) The decay kinetics of self-trapped (ST) excitons in one-dimensinal conjugated polymers were explained with a model in which potential crossing and tunneling between two potential curves of the ST exciton and the ground state are the major processes in the relaxation. The weak temperature dependence indicates that the activation process over the potential barrier between the ST exciton and the ground state is not dominant in the radiationless relaxation of the ST exciton.

(2) Geometrical relaxation of main chain configuration in PDA was also investigated by time-resolved Raman gain spectroscopy with 300 fs resolution which is the highest time resolution of the vibrational spectrum ever reported. The Raman signal due to the ST exciton in PDA was observed at 1200 cm^{-1}. The observed Raman signals offer most direct evidence of the structure of ST exciton being butatriene-like structure after geometrical relaxation from acetylene-like structure in free exciton state.

(3) The stimulated Raman gain signals of a single-crystal PDA-DFMP, with the sidegroups 2,5-bis trifluoromethyl-phenyl, were reported to exhibit an optical Stark shift of about 50 cm^{-1}. Using an ultrashort, near-resonant high intensity laser, the intensity dependent signal shifts to higher probe photon energies for both the C=C and C≡C stretching modes. Semi-quantitative agreement between the data and a 3-level system density matrix calculation is achieved using a nonlinear optical mechanism in which a pump laser field is optically coupled to both the exciton ← zero-phonon ground state and the exciton ← one-phonon ground state transitions.

1. INTRODUCTION

The latter-half of the twentieth century is marked by the development of electronics based on semiconductor industry and technology. The speed and memory in computers will reach the limit, which will not be sufficient in near future. Since the bandwidth of optical wave is much broader than that available with electronics, the next century is expected to be an "Optopia", where extensive development of optronics and/or photonics is to be attained. The industry of the early stage of optronics or photonics, namely, opto-electronics, has been developed for the last ten years and the gross products of this industry in 1992 in the author's country, Japan, is reported to have exceeded five trillion yen. In order for the industry of optronics or photonics to realize the optopia, the search for the nonlinear optical materials is of key importance.[1] The properties of the materials for the information processing and memory storage should satisfy some or all of the following requirements. (1) Large third-order optical nonlinearity. (2) Ultrafast nonlinear response. (3) Low absorption, reflection, and scattering loss at operation wavelengths. (4) Possibility of manufacturing waveguide. (5) Long-term stability of nonlinear susceptibility and dynamics. (6) Stability and absence of degradation at the operational level of lasers. From these viewpoints there are a few groups of materials attracting scientists in the field.

Among others conjugated polymers seem to be promising candidates for future practical applications in nonlinear optical devices. Because of their often large nonlinear optical susceptibilities and their role as model compounds for quasi-one-dimensional semiconductors. Considerable interest has been directed to the electrical and optical properties of polymers with long conjugated chains such as polyacetylenes(PA), polydiacetylenes(PDA), polythiophenes(PT), polypyrrole, polythienylenevinylene(PTV), polyphenylene(PP), and polyphenylenevinylene (PPV).[1-23] Figure 1.1 shows the molecular structures of these polymers. The major differences in the electronic and optical properties among these polymers lie in the backbone structure. For example PA possesses the conjugated polyene type (-CH = CH-)$_n$ main chain, PDAs have the diacetylene-type configuration (=CR-C=-C-CR=)$_n$ with both double and triple bonds, and PTs, PTV, PP, and PPV contain ring structures in their repeating units.

It is of great interest to study the kinetics of excitations in PDAs, PTs and PTV and compare the results with those of PA, especially the formation and decay processes of solitons in PA and ST excitons in PDAs and PTs. The kinetics of photoexcitations have been studied in a polydiacetylene-toluene-sulfonate (PDA-TS) single crystal. The population decay time was measured to be less than 2 ps by transient absorption spectroscopy,[24] and by degenerate four-wave mixing in a PDA-TS single crystal.[25] In nanosecond time-resolved reflection spectroscopy studies, decay kinetics represented by erf[$(t/\tau)^{-1/2}$] with $\tau=1.0$ μs has been reported. [23,26] The decay kinetics was explained in terms of the geminate recombination of a pair of excitations after random walks in one-dimensional chains.[27] The photoexcitations in the nanosecond region were assigned to photoinduced polarons.

2. RESULTS AND DISCUSSION

2.1. Mechanism of exciton self-trapping in one-dimensional system

From the extensive experimental study of polymers in our group, the following model to describe the self-trapping process of free exciton and decay dynamics of the self-trapped exciton is proposed.

Fig.2.1.1 shows the potential curves of free and self-trapped excitons in one-dimensional conjugated polymers. Since there is no barrier in the potential curve between free and ST excitons in an ideal one-dimensional system, the formation of the ST excitons is expected to take place within the period of the coupled phonon cycle $T_M = 2\pi/\omega_M$, The experimental results of the absorption spectra, the Raman gain [27-29], the resonance Raman scattering, and the phonon-mediated optical nonlinearity show that the singlet excitons in polydiacetylenes are coupled with the C=C and C≡C stretching modes. The coupled stretching mode frequencies are about 1500 cm^{-1} (C=C stretching) and 2100 cm^{-1} (C≡C stretching) and correspond to oscillation periods of 20 and 15 fs, respectively. Both of them are much shorter than the experimentally observed appearance times of ST excitons, which are 150 fs in PDA-3BCMU, 100 fs in PDA-4BCMU, 70 fs in P3MT, and 100 fs in P3DT.
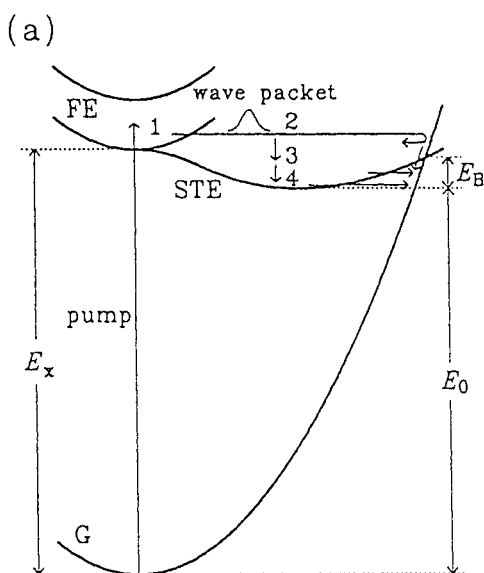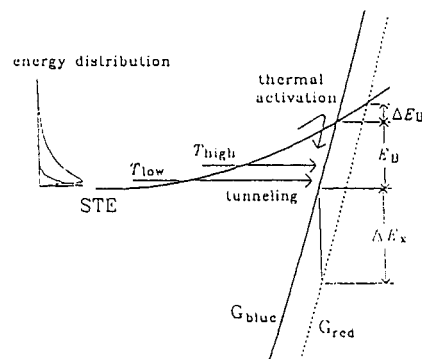

Fig. 2.1.1. A model of the relaxation kinetics and the dependence on exciton energy shown in the potential surfaces of excitons in PDA. State 1, 2 and 3, 4and 5 are free exciton (FE), nonthermal self-trapped exciton (STE), quasithermal STE, and thermal STE, respectively. G_{blue} and G_{red} are ground states of blue-phase PDA and red-phase PDA, respectively.

In the following, the terminology "self-trapping" is used in two ways. One is the change in the potential curve of excitons which have the same energy as the free excitons. The self-trapping time estimated above from the oscillation period is used in this meaning. The other is the emission of phonons of the most strongly coupled mode to the excitonic transition. After this process the exciton energy is lower than that of the free exciton, and the population of the ST excitons is distributed near the bottom of the "ST" exciton (STE) potential in Fig. 2.1.1.

According to Jortner,[30] the rate of the self-trapping process of the second meaning in rare gas solids such as Ne and Ar at low temperatures is given by $k_{ST} = \omega_M \exp(-\omega_M/\omega_D)$, where ω_M and ω_D are the frequencies of the most strongly coupled mode and the Debye frequency, respectively. Using the values of ω_D in literature and ω_M given above, the calculated rate k_{ST} is several orders of magnitude smaller than the observed rate in the polymers.[27,28] This is because of the too simple phonon structure in the model only suited to the rare gas solids. Much longer self-trapping time can be explained by the geometrical reorganization (relaxation) involving the lower frequency modes than the oscillation period of the strongly coupled modes. The lower frequency modes may include those associated with the structural change in the bulky side chains, which are lacking in the rare gas solids.

There is difference in the formation time of ST excitons, namely "self-trapping" time of the second meaning, between PDAs and PTs. The formation times are 150 fs in PDA-3BCMU and 140 fs in PDA-4BCMU in the blue phase and 70 fs in P3MT and 100 fs in P3DT. This can be explained by the difference in the chemical structures of these two groups of polymers. PDA-3BCMU and PDA-4BCMU have side groups with hydrogen bonds connecting neighboring side chains, while P3MT and P3DT have rigid structures of thiophene rings conjugated with each other. The side chains of PTs have the helical noncoplaner structure due to the steric hindrance among the side groups.[31,32] The van der Waals

interaction between the side chains and that between main chain and side chains are more intense in P3DT than in P3MT because of the longer side group in the former. This explains the longer formation time in the former.

The self-trapping time constant of excitons in P3MT is 70 fs, which is different from 150 fs in PDA-3BCMU only by a factor of two although the differences in the structure and size of the side chains are very large. This may be due to the following three possible mechanisms. Mechanism (1); Finite time is needed for the self-trapped exciton to slide down along the adiabatic potential because the potential curve of the self-trapped exciton deviates from the free- exciton potential bottom, which is flat with null derivative.[33,34] Mechanism (2); According to Sumi's theory concerning the self-trapping process in reduced dimensionalities,[34] the spontaneous geometrical relaxation, which takes place from infinitely extending free exciton to the self-trapped exciton, follows a reaction pathway with very small slope along the reaction coordinate. Mechanism (3); Because of the interchain interaction, the conjugated polymers may not be an ideal one-dimensional system. Then there may be a low barrier between two minima in the potential curves of the ground state and the ST exciton state.

2.2. Decay mechanism of self-trapped excitons in conjugated polymers

In this subsection the following properties are addressed concerning the excited state dynamics in conjugated polymers, especially polydiacetylenes.

(1) Many of conjugated polymers are nonfluorescent or only weakly fluorescent. Especially the quantum efficiency of the nonfluorescent blue form of polydiacetylenes is estimated to be lower than 10^{-5} and that of the fluorescent red-phase polydiacetylenes is only of the order of 10^{-4}.

(2) There are common features in the transient absorption spectra of both PDAs (blue-phase PDA-3BCMU and PDA-4BCMU and red-phase PDA-4BCMU) and PTs either in random films or in oriented films. One feature is very broad absorption spectra in 1.35-1.9 eV region observed just at excitation (0 ps).

(3) Triplet exciton cannot be formed directly from the singlet exciton. They are formed only at high density excitation of exciton transition or by charge carrier creation by the interband transition.

(4) The formation and decay times and photoluminescence properties of the ST excitons in several PDAs and PTs studied are summarized in Table 2.2.1.

Table 2.2.1: The formation time (τ_f) and the decay time*1 (τ_d) of self-trapped (ST) excitons and fluorescence property of several polymers

polymer	τ_f(fs) (290K)	τ_d(ps) (10K)	τ_d(ps) (290K)	fluorescence property*2
PDA-3BCMU (blue,oriented film*3)	150±40	1.9±0.2	1.6±0.1	n
PDA-3BCMU (blue,cast film)	150±50	2.0±0.2	1.5±0.2	n
PDA-DFMP (blue,single crystal)	100±30	---	1.6±0.1	n
PDA-4BCMU (blue,oriented film)	140±50	2.1±0.1	1.6±0.1	n
PDA-4BCMU (red,oriented film)	120±60	0.96±0.09*4	---	wf
PDA-4BCMU (red,cast)	<200	0.88±0.08*4	---	wf
P3MT (electrochemical preparation)	70±50	0.62±0.07*4	---	wf
P3DT (electrochemical preparation)	100±50	0.45±0.06*4	---	wf

*1 The formation of ST exciton corresponds to the emission process of strongly coupled phonon to the excitonic transition.
*2 Polymers with about 10^{-4} and lower fluorescence quantum efficiency than 10^{-5} is indicated by wf (weakly fluorescent) and n (nonfluorescent), respectively.
*3 The sample is prepared by the polymerization of evaporated monomer film of PDA-3BCMU on a KCl crystal. The sample is composed of small crystals and amorphous regions.
*4 This decay time is determined by the initial slope of the semilogarithmic plot in the early delay time shorter than 1ps.

Figure 2.2.1 shows the time dependence of the absorbance change due to the self-trapped excitons in several PDAs and PTs, after the component, which does not decay within 150 ps, being subtracted. As can clearly be seen in the figure, the decay of nonfluorescent PDA-3BCMU in the blue phase and PDA-4BCMU in the blue phase are approximately given by an exponential function except the early stage within 500 fs. The other fluorescent polymers have nonexponential decay from very early delay time until 30 ps. The initial decay times defined by the slope of the semilogarithmic plot of the absorbance change against delay time just after excitation are determined as 890±160 fs, 620±60 fs, and 450±50 fs in PDA-4BCMU, P3MT, and P3DT, respectively, at 10 K. The decay becomes slower and slower at longer delay times because of the less efficient tunneling due to the thicker barrier width through which the population of excitons must tunnel to relax to the ground state.

The lifetime of the self-trapped ^1B_u excitons in PDA-3BCMU is much shorter than the radiative life (a few ns) estimated from the oscillator strength of the transition. This means predominant radiationless relaxation in the exciton decay process. Excitons in many semiconductors and organic molecular crystals have lifetimes between several hundred picoseconds and several hundred nanoseconds at low temperatures. More than one order of magnitude differences in the lifetime of these excitons are usually found between low temperatures and room temperature. The activation potential barrier is very often invoked to explain the temperature dependence in most excitons in semiconductors, organic molecular crystals, and also in ionic crystals.
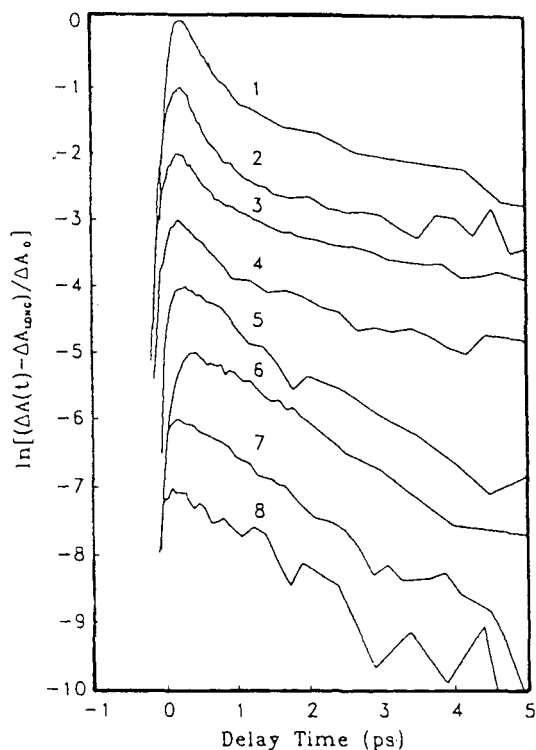
Fig. 2.2.1. Time dependence of the absorbance change due to the self-trapped excitons in several PDAs and PTs, after the very long-life component being subtracted. The decay curves from the top to the bottom correspond to 1. P3MT (observed at 10K at the probe photon energy of 1.63 eV); 2. P3DT (10K, 2.34 eV); 3. PDA-4BCMU (red-phase cast film, 10K, 1.77 eV); 4. PDA-4BCMU (blue-phase oriented film, 10K, 1.77 eV); 5. PDA-4BCMU (blue-phase oriented film, 290K, 1.77 eV); 6. PDA-3BCMU (blue-phase cast film, 290K, 1.77 eV); 7. PDA-3BCMU (oriented single crystals and amorphous domains prepared by evaporation on a KCl single crystal surface (100), 290K, 1.77 eV), and 8. PDA-DFMP (297K, 1.98 eV). The excitation pulse width and energy are 100fs and 1.97 eV, respectively. The samples of PDA-4BCMU in red-phase are excited by the two-photon process.

The relaxation of photoexcitations in polymers in general can be described as follows using PDAs and PTs as examples.[27-29,35] The differences in the relaxation kinetics of excitons in the nonfluorescent PDA-3BCMU and PDA-4BCMU in the blue phase and fluorescent PDA-4BCMU in the red phase and P3DT and P3MT are discussed. The discussion is based on the Toyozawa's theory.[36,37] Figures 2.2.2 and 2.2.3 show the potential curves of the ground state (G) and self-trapped exciton (STE), and free exciton (FE) band of the nonfluorescent (Fig. 2.2.2) and fluorescent (Fig. 2.2.3) polymers, respectively. The curvature of the potential of STE is larger than those of G and FE states in order to take into account the discussion on the reaction coordinate by Sumi et al.[34] and the small Stokes shift of fluorescent polymers. The electronic structure of the polymer systems are too complicated to be represented by the one-dimensional potential curve. The small Stokes shift may also be explained by the ground-state potential having two minima with a small barrier between two configurations corresponding to the acetylenic and butatrienic resonance structures or to the aromatic and quinoid resonance structures in the cases of PDAs and PTs, respectively.

In Figs. 2.2.2 and 2.2.3, the self-trapping process from FE (indicated by the number 1 in the figures) to STE (indicated by 2) is the process 1 - 2, followed by the emission of phonon of strongly coupled modes to the excitonic transition.

The STEs after the phonon emission process still remain in the nonthermal states (3). The nonthermal STEs (3) are coupled with phonon modes (intrachain vibrations) of low frequencies and thermalize to states, where temperatures of the intrachain vibration can be defined. The thermalization process (3 - 4) is observed as the spectral change at delay times from 0.5 ps to 5.0 ps. The time constant of the thermalization can be determined by the time dependence of absorbance change ratio among several different wavelengths. The obtained time constant of the thermalization process is about 1 ps in both red-phase PDAs and P3DT. However, the temperature of the STEs defined from equilibrated vibrational modes after this 1-ps thermalization process may be still higher than the bulk temperature of the polymer sample. Therefore, the cooling down process (4 - 5) with a time constant of several or a few tens picoseconds is expected to take place after the observed thermalization process. However the spectral change due to the cooling down process of the STEs could not be clearly detected in this study because of limited signal to noise ratio of the spectral data.

The change of the decay rate observed in the red-phase PDA-4BCMU and P3DT can be explained by the competition between the thermalization and tunneling processes. The STEs relax to the ground state mainly by tunneling through the barrier between the STEs and ground-state potentials. The initial fast decay is the relaxation from the nonthermal and quasi-thermal STEs (indicated by 3 - 4 in Fig. 2.2.3) with the time constant of about 1 ps or slightly less. After the thermalization the STEs come down close to the bottom of the potential and the loss rate by the tunneling becomes slower because of the increase in the barrier height and thickness. The decay time constant of about 5 ps is due to the tunneling from the thermal STE (indicated by 4 in Fig. 2.2.3). The thermalization process of the STE is estimated as about 1 ps from the spectral change. The wavelength dependence of the decay curve can be explained by

the thermalization process. The absorbance change at 2.00 eV in the red-phase PDAs is mainly due to the quasi-thermal STEs and the thermal STEs have the absorption peak at 1.6 eV. Therefore, the decay curve at 2.00 eV can be fitted to a single exponential function with the time constant of about 1 ps. The time constant of the absorbance change below 1.8 eV is longer than that of the bleaching, because the quasi-thermal STEs thermalize with the time constant of 1 ps and the absorption peak due to the thermal STEs appears at 1.6 eV. The observed data for P3MT and P3DT can be explained in the same way.
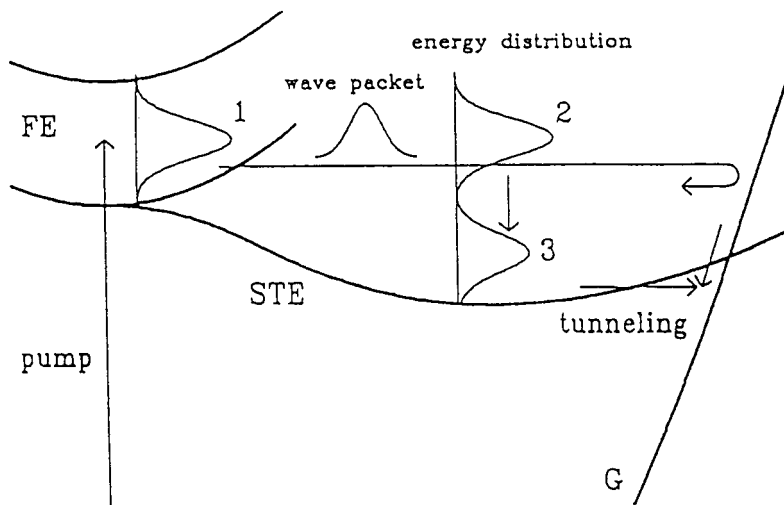

Fig. 2.2.2. Potential curves of the ground state (G), free exciton (FE), and self-trapped exciton (STE) of the nonfluorescent PDAs with fluorescence efficiency lower than 10^{-5}. The meanings of numbers 1, 2, and 3 are the same as in Fig.2.1.1.
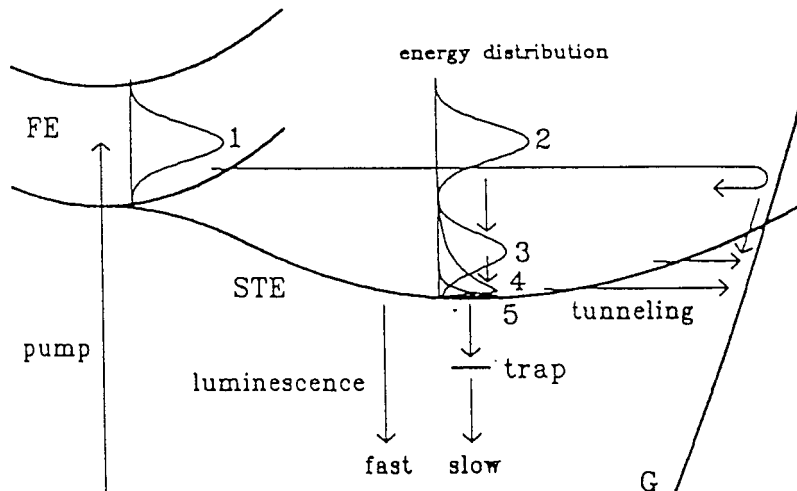

Fig. 2.2.3. Potential curves of the ground state (G), free exciton (FE) band, and self-trapped exciton (STE) of the very weakly fluorescent PDAs with fluorescence quantum efficiency of about 10-4 or slightly more. Numbers 1, 2, and 3 are the same as in Fig. 2.1.1. Number 4 means STE after thermal equilibration among intramolecular vibrational modes to a local temperature, which is higher than the bulk experimental temperature of the samples. Number 5 indicates the STE after the local temperature is lowered to the bulk experimental temperature.

The change of the decay rate observed in the red-phase PDA-4BCMU and P3DT can be explained by the competition between the thermalization and tunneling processes. The STEs relax to the ground state mainly by tunneling through the barrier between the STEs and ground-state potentials. The initial fast decay is the relaxation from the nonthermal and quasi-thermal STEs (indicated by 3 - 4 in Fig. 2.2.3) with the time constant of about 1 ps or slightly less. After the thermalization the STEs come down close to the bottom of the potential and the loss rate by the tunneling becomes slower because of the increase in the barrier height and thickness. The decay time constant of about 5 ps is due to the tunneling from the thermal STE (indicated by 4 in Fig. 2.2.3). The thermalization process of the STE is.

estimated as about 1 ps from the spectral change. The wavelength dependence of the decay curve can be explained by the thermalization process. The absorbance change at 2.00 eV in the red-phase PDAs is mainly due to the quasi-thermal STEs and the thermal STEs have the absorption peak at 1.6 eV. Therefore, the decay curve at 2.00 eV can be fitted to a single exponential function with the time constant of about 1 ps. The time constant of the absorbance change below 1.8 eV is longer than that of the bleaching, because the quasi-thermal STEs thermalize with the time constant of 1 ps and the absorption peak due to the thermal STEs appears at 1.6 eV. The observed data for P3MT and P3DT can be explained in the same way.

The decay of the nonthermal (but relaxed, namely after large frequency phonon emission) STE in blue-phase PDAs is faster than in red-phase, because the crossing point is lower than the point in red-phase PDAs. The major part of the STEs relax to the ground state before thermalization. The decay rate from the nonthermal STEs to the ground state is not much slower than the decay rate from the quasi-thermal STEs. Therefore, the decay curves in the blue-phase PDAs can be fitted to single-exponential functions. The wavelength dependence of the time constant is due to the mixed signals of the STE states. The bleaching signal exhibits the unrelaxed and relaxed (i.e. after large frequency phonon emission) but nonthermal STEs, while the absorption around 1.8 eV is due to the unthermalized STEs. Therefore, the observed decay time constant of the bleaching is shorter.

The difference between fluorescent and nonfluorescent polymers is in the time constants of the tunneling from the nonthermal and quasi-thermal STEs to the ground state. The time constants in the blue-phase PDAs are between 1 ps and 3 ps and they are shorter than that in the red-phase PDAs. Therefore the number of the remaining STE at the bottom of the STE potential curves in the blue-phase PDA is smaller and the luminescence could not be detected. The fast component of the luminescence in the red-phase PDAs is considered to be due to the free excitons and/or STEs and the slow component is due to the traps in the polymer chains. The detailed study using highly oriented samples is also consistent with the above model.[38]

The proposed relaxation model predicts that the decay rate of the STE in conjugated polymers depends on the exciton energy. Conjugated polymers with large exciton energy are considered to have excitons with long lifetime and to be more fluorescent. For example poly(*p*-phenylenevinylene)(PPV), which has an absorption peak at 2.5 eV has strong luminescence with a quantum yield of several percent.[39,40] Much higher fluorescence quantum efficiency of PPV than red-phase PDAs may also be due to non-ideal one dimensionality in the polymer, caused by interchain interaction because of small side groups.

Recently, a Langumuir-Blodgett film of PDA-(12,8), which has an exciton peak at 1.88 eV, has been studied and the decay time constant of the STE is estimated as 1.3±0.1 ps at 290 K.[41] It is shorter than that in blue-phase PDAs which have an exciton peak at 1.97 eV. These results are consistent with the above proposed model. However, PDA under the hydrostatic pressure has different decay kinetics. When the pressure increases, the absorption edge of red-phase PDA-4BCMU shifts to lower energy but the decay kinetics becomes slower.[42] This pressure effect is probably due to a subsequent three-dimensional distortion of the polymer chain. The decay kinetics under the pressure may be different from that in the one-dimensional system.

Thus low fluorescence quantum efficiency of the one-dimensional polymers is systematically explained by the proposed model shown by Figs. 2.2.2 and 2.2.3. While in fluorescent PDA-4BCMU in the red phase and P3MT and P3DT, the crossing points are higher than in PDA-3BCMU and PDA-4BCMU in the blue phase because of the higher energy of free and ST excitons. In the red phase PDA-4BCMU a larger fraction (probably 10 to several tens %) of free excitons are relaxed to ST excitons with 3 ps lifetime at 10 K. This is shown in Figs. 2.2.2 and 2.2.3 as fast tunneling through and passing through the crossing point of the potential curve between the ST exciton and the ground state. The ratio of the contribution of the tunneling and activation processes must be determined for each polymer by detailed experiments of the temperature dependence of the primary decay kinetics. The time constants of the various relaxation processes in three polymers are listed in Table 2.2.2.

Table 2.2.2: Time constants of the relaxation processes of excitons at 290 K

Relaxation processes[1]	PDA-4BCMU(blue) (oriented film)	PDA-4BCMU(red) (oriented film)	P3DT
1 - 2 (self-trapping)[2]	(10-20 fs)	(10-20 fs)	(10-20 fs)
2 - 3 (phonon emission)	140±40 fs	120±60 fs	100±50 fs
3 - 4 (thermalization)	---[3]	1.1±0.1 ps	1.0±0.2 ps
2 - G (tunneling from unrelaxed STE)	< 1.0 ps		
3 - G (tunneling from nonthermal STE)	1.6±0.1 ps	0.7±0.1 ps[4]	0.3±0.1 ps[4]
4 - G (tunneling from thermal STE)	----[5]	4.4±0.5 ps[6]	4.7±1.2 ps[6]

[1] 1-4, and G are the states shown in Figs. 2.2.2 and 2.2.3.
[2] The time constants of the self-trapping processes could not be time-resolved in this study.
[3] The thermalization process could not be detected in the blue-phase PDA.
[4] The tunneling processes from the unrelaxed STE and from the nonthermal STE could not be separated.
[5] The tunneling from thermal STE in the blue-phase PDA-4BCMU could not be observed because the nonthermal STEs disappear before thermalization.
[6] The decay times are determined by the absorbance change at lower delay time than 5ps.

2.3. Temperature dependence of decay kinetic

The photoinduced absorbance changes (ΔA) at 0.5 ps in PDA-(12,8) LB films are shown in Fig. 2.3.1 with the pump spectra. Bleaching due to absorption saturation and broad photoinduced absorption below the absorption edge are observed. The photoinduced absorption has two peaks at 1.4-1.6 eV and just below the absorption edge. The peak around 1.4-1.6 eV and that near the absorption edge are assigned to the transitions from the lowest ^1B_u exciton to m^1A_g (m>1) excitons and to composite exciton state, i.e. biexciton with ^1A_g symmetry, respectively.[35]
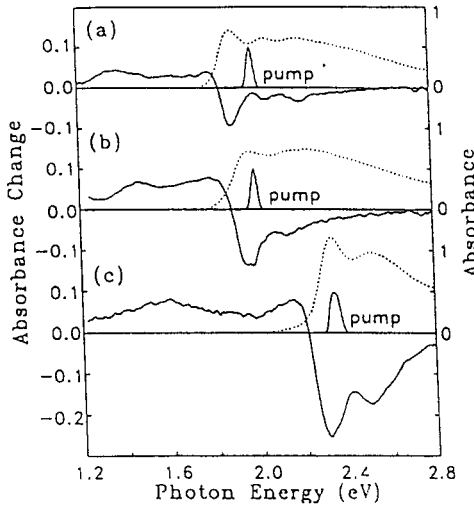

Fig. 2.3.1. Transient absorption spectra at 0.5 ps in PDA LB films at 290 K. (a) PDA-(12,8)-PAA, (b) blue-phase PDA-(12,8)-Cd, and (c) red-phase PDA-(12,8)-Cd. The absorption (dotted curves) and pump spectra are shown together. The pump photon densities are (a) 9.2×10^{14}, (b) 1.8×10^{15}, and (c) 2.5×10^{15} photons/cm^2.

The transient absorption spectra in PDA-(12,8)-PAA are shown in Fig. 2.3.2. The sharp bleaching peak at 1.88 eV and associated two peaks at 2.04 and 2.18 eV are due to the saturation of the excitonic absorption and the phonon side bands, respectively. At 0.0 ps, three small minima due to Raman gain are clearly seen at 1.71, 1.62, and 1.44 eV. The corresponding Raman shifts, 2100, 2820, and 4270 cm^{-1}, are assigned to the stretching vibration of the C≡C bond and the overtone of the C=C bond and the C≡C bond, respectively. The coherent coupling between pump polarization and probe field which has been observed at the pump photon energy in blue-phase PDAs in our previous paper[27,41] is not clear, because of the complexity introduced by the location of the pump photon energy between the lowest exciton peak and the phonon side band. The photoinduced absorption at 0.0 ps is larger at lower probe photon energies down to 1.2 eV. Then the absorption has two peaks at 1.4 and 1.8 eV at delay times longer than 0.2 ps. The time constant of this spectral change is determined as 120±50 fs from the transient response at 1.8 eV. A similar spectral change with a time constant of about 150 fs is also observed in blue- and red-phase PDA-(12,8)-Cd LB films and other PDAs.[27,28,35,41,43]
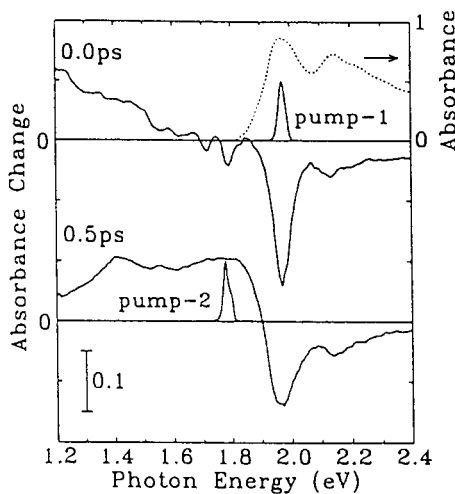

Fig. 2.3.2. Transient absorption spectra of PDA-(12,8)-PAA at 290 K. The absorption (dotted curve) and pump spectra are shown together.

The transient responses of the bleaching in the PDA LB films are plotted in a semilogarithmic scale in Fig.2.3.3. Here, long-lived components (ΔA_c) due to triplet excitons are subtracted from the observed absorbance changes.[43] The decay curves do not fit with a single-exponential function. The decay times defined by the initial slope of the semilogarithmic plot between 0.2 and 0.6 ps are shorter than 1 ps, and ΔA decays more slowly after this rapid decay.

The time constants defined by the decay curves at delay times longer than 2 ps are summarized in Table 2.3.1. The decay time constant becomes shorter at higher temperatures and in PDA with smaller exciton energy.

Table 2.3.1: Decay time constants obtained from the data at delay times longer than 2 ps in PDA-(12,8) LB films at several temperatures.

PDA LB films	Exciton Energy E_x (eV)	Decay Time Constant (ps)			
		10 K	100 K	200 K	290 K
(a) PDA-(12,8)-PAA	1.88	1.8±0.1	1.7±0.1	1.5±0.3	1.3±0.1
(b) PDA-(12,8)-Cd (blue)	1.97	2.1±0.1	1.8±0.1	1.6±0.1	1.5±0.1
(c) PDA-(12,8)-Cd (red)	2.32	6.1±1.2	4.2±0.5	3.9±0.6	3.3±0.5

Since the ultrafast relaxation processes in PDAs are insensitive to the sample morphology,[43] the exciton energy dependence of the decay kinetics can be discussed using a model shown in Fig.2.1.1. Here, the potential curves of free exciton (FE) and self-trapped exciton (STE) are assumed to be independent of the exciton transition energy E_x. Polyenes have the 2^1A_g state below the 1^1B_u state,[44] but the 2^1A_g state in longer polyene systems is expected to separate to form two ^3B_u states.[45] The observed long-lived triplet excitons in PDAs are not created directly via the 1^1B_u exciton generated by single photon excitation of the 1.97 eV pump pulse, but created by fission of a higher excited singlet exciton generated by the Auger process of two 1^1B_u excitons.[46] Therefore, the relaxation rate from the 1^1B_u exciton to the 2^1A_g exciton is considered to be much smaller than the relaxation rate to the ground state. The 2^1A_g state in PDA can be neglected in the ultrafast relaxation of the 1^1B_u exciton.

Time Dependence of Absorbance Change
PDA-(12,8) LB films 290K

$W_c^{-1} = 0.98±0.28 ps$ $\alpha^{-1} = 0.066±0.016 eV$

$\Delta E_b/\Delta E_x = 0.15±0.03$

$E_b = 0.04 eV (PAA), 0.05 eV (Cd blue), 0.11 eV (Cd red)$

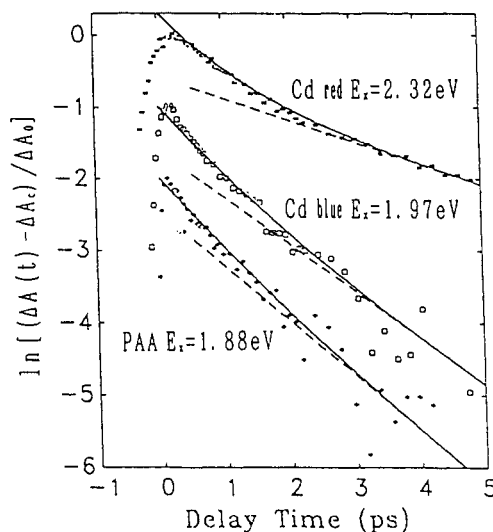$E_t - E_0 = 0.26 eV$ (stabilization energy of STE)

Fig. 2.3.3. The time dependence of the absorbance changes in PDA LB films at 290 K plotted in a semilogarithmic scale. (a) PDA-(12,8)-PAA (solid circles), (b) blue-phase PDA-(12,8)-Cd (open squares), and (c) red-phase PDA-(12,8)-Cd (solid squares). The probe photon energies are (a) 1.88 eV, (b) 1.94 eV, and (c) 2.30 eV. Dashed lines are single-exponential functions obtained from the data at delay times longer than 2 ps. Solid curves are decay kinetics simulated using eqs. (16)-(18) with $T_0 = 3000$ K.

The spectral change of the photoinduced absorption with a time constant of about 150 fs is due to the geometrical relaxation of FE to STE. Since the formation process of STE has no barrier in one-dimensional system, the photoexcited FE (state 1) is coupled with the C-C stretching modes within the phonon periods of 10-20 fs. However, STE has not relaxed to the bottom of the potential curve and the stabilization energy remains as the kinetic energy of the lattice vibration (nonthermal STE (state 2)). The nonthermal STE then relaxes to quasithermal STE (state 3) coupled with vibrational modes within a single chain of polymer. The observed spectral change with a time constant of about 150 fs is considered to be due to this process. Slow spectral change with a time constant of 1.1±0.1 ps observed

in red-phase PDA-4BCMU corresponds to relaxation from quasithermal STE to thermal STE (state 4).[41] There are three possible mechanisms of nonradiative relaxation in the decay kinetics from STE to the ground state as shown in Fig.2.1.1(b), i.e. (1) thermal activation, (2) multiphonon transition, and (3) tunneling in configuration space.

(1) If the relaxation from STE to the ground state is mainly due to passing through the crossing point shown in Fig. 2.1.1(b)(1), the temperature dependence of the decay rate is given by

$$R_a(T) = R_{ao} \exp(-E_B/kT), \tag{2.3.1}$$

where E_B is the activation energy to pass through the crossing point and R_{a0} is the frequency of the activation process. Using the data in Table 2.3.1, E_B and R_{ao}^{-1} in PDA-(12,8) LB films are obtained as (a) 0.18 meV (2.1 K) and 1.5 ps, (b) 0.24 meV (2.8 K) and 1.6 ps, (c) 0.45 meV (5.2 K) and 3.7 ps, respectively. The weak temperature dependence gives very small activation energy. The fastest decay rate in the activation process ($kT \gg E_B$) is R_{a0}, but the observed initial decay rate is faster than the obtained decay rate R_{a0}. Therefore, the relaxation via the crossing point is concluded not to be a major relaxation process.

(2) The ultrafast nonradiative decay in cis-polyacetylene was once explained by multiphonon transition.[47] The temperature dependence of the multiphonon transition rate is approximately given by

$$R_m(T) \propto \left[\frac{1}{\exp(\hbar\omega/kT)-1} + 1 \right]^{E_0/\hbar\omega}, \tag{2.3.2}$$

where $\hbar\omega$ is phonon energy and E_0 is the energy difference between the bottoms of the STE potential curve and the ground state.[48] Since the corresponding temperature of the phonon energy in PDA is much higher (0.19-0.26 eV = 2200-3000 K) than the experimental temperature, the difference between multiphonon transition rates at 10 and 290 K is very small and estimated to be less than 1%. Therefore, the multiphonon transition is not a main relaxation process.

(3) The main relaxation process from STE to the ground state is considered to be due to tunneling in the configuration space from the STE potential to the ground state (Fig.2.1.1(b)(3)) and the following phonon emission process from high vibrationally excited levels of the ground state. The nonradiative transition probability from the excited state |j,x> to the ground state |j+p,g> with the same energy, where both j and j+p specify the vibrational levels, was calculated considering the overlap of vibrancy wavefunctions.[49,50] The transition rate was obtained as

$$W_j = C |<j,x|j+p,g>|^2$$
$$= C \exp(-S)S^p \frac{j!}{(j+p)!} [L^p_j(S)]^2, \tag{2.3.3}$$

where C is a physical factor, $p=E_0/\hbar\omega$, $S=(E_x-E_0)/\hbar\omega$, and L^p_j is the Laguerre polynomial. Since S and j in PDA are expected to be much smaller than p (S, j<<p), the transition rate is approximately given by

$$W_j \sim W_0 \frac{(j+p)!}{j!p!} \sim W_0 p^j \qquad (j = 0\text{-}1). \tag{2.3.4}$$

This is consistent with the tendency that STE with higher energy from the bottom of the potential curve has faster tunneling rate because of narrower barrier width. Since STEs in conjugated polymers are coupled with both intrachain and interchain phonon modes, the STE energies are expected to be distributed continuously. Therefore, the transition rate of STE with energy E is assumed as

$$W(E) = W_0 \exp(\alpha E) = W_C \exp[\alpha(E-E_B)] \qquad (E<E_B)$$
$$W(E) = W_0 \exp(\alpha E_B) = W_C \qquad (E>E_B), \tag{2.3.5}$$

where $\alpha = \log p/\hbar\omega$. W_C is the transition rate of STE with the energy larger than the crossing point and is assumed to be constant and independent of the exciton transition energy. The energy distribution of the thermal STE is defined by the temperature. At higher temperatures the thermal STEs are distributed to higher energies and the transition rate is faster. The relaxation rate of STEs at temperature T is calculated as

$$R_t(T) = \frac{\int_0^\infty n(E)W(E)dE}{\int_0^\infty n(E)dE}$$
$$= W_C \frac{\exp(-\alpha E_B)-\alpha kT \exp(-E_B/kT)}{1-\alpha kT}, \tag{2.3.6}$$

where the distribution of exciton, n(E), is assumed to be exp(-E/kT). Since the position of the ground state shown in Fig.2.1.1 depends on the exciton energy E_x, the height of the crossing point depends on the exciton energy. When the exciton energy increases by ΔE_x (solid curve G_{blue} to dotted curve G_{red} in Fig.2.1.1(b)), the crossing point becomes higher by ΔE_B. When the change in the exciton energy is small, the barrier height is given by

$$E_B = \frac{\Delta E_B}{\Delta E_x} (E_x - E_{x0}) .$$

(2.3.7)

The parameters are determined by the least-square fitting using the data in Table 2.3.1 as $W_C^{-1} = 0.98\pm0.28$ ps, $\alpha^{-1} = 0.066\pm0.016$ eV, $\Delta E_B/\Delta E_x = 0.15\pm0.03$, and $E_{x0} = 1.62 \pm 0.14$ eV. E_{x0} means the exciton transition energy with zero barrier height. However, Eq. 2.3.7 is not a good approximation for $E_x \sim E_{x0}$. The actual exciton energy with zero barrier height is smaller than the obtained E_{X0}. The value of α^{-1} is calculated from the relation between Eqs. 2.3.4 and 2.3.5 using p=10 and $\hbar\omega$=0.19 eV as 0.083 eV. This is consistent with the value obtained from the experimental results. The potential barrier height (E_B) and the relaxation time from the bottom of the STE potential curve (W_0^{-1}) in PDA-LB films are obtained, respectively, as (a) 0.04 eV and 1.8 ps, (b) 0.05 eV and 2.1 ps and (c) 0.11 eV and 5.2 ps. The decay time constant in yellow-phase PDA with exciton energy of 2.6 eV is calculated as 6.2 ± 2.1 ps at 293 K. This is consistent with the fluorescence lifetime of 9 ± 3 ps obtained in PDA-3KAU yellow-phase solution.[51] The main relaxation process of STE is concluded to be due to the tunneling in the configuration space.

The time dependence of the bleaching shown in Fig. 2.3.3 can be explained by the thermalization processes of STE. Since the pump pulse excites the excitonic absorption peak, the distribution of the nonthermal STE is defined as $N_{nonth}(E) = \delta[E - (E_x - E_0)]$. Then the nonthermal STE relaxes to the quasithermal STE with time constant $\tau_{nonth} = 150$ fs. The temperature of the quasithermal STE decreases with time constant of $\tau_{quas} = 1.1$ ps and the relaxation rate to the ground state becomes slower. Therefore, the rate equations for the populations and temperature change are given by

$$\frac{dN_{nonth}}{dt} = - [W(E_x-E_0) + \frac{1}{\tau_{nonth}}] N_{nonth}$$

(2.3.8)

$$\frac{dN_{quas}}{dt} = \frac{N_{nonth}}{\tau_{nonth}} - R_t(T)N_{quas}$$

(2.3.9)

$$T = T_0 \exp(-t/\tau_{quas}) + T_{therm} ,$$

(2.3.10)

where N_{nonth} and N_{quas} are the populations of nonthermal STE and quasithermal STE, respectively, T_{therm} is the experimental temperature, and the initial temperature increase, T_0, is assumed to be $(E_x-E_0)/k$ from the stabilization energy of STE. Since the population of thermal STE corresponds to N_{quas} at T_{therm}, the photoinduced bleaching signals are proportional to the sum of N_{nonth} and N_{quas}. The calculations with $T_0 = 3000$ K give good fitting curves for each The PDA, as shown in Fig. 2.3.3. The stabilization energy E_x-E_0 is determined as 0.26 eV. It is larger than the potential barriers in both blue- and red-phase PDAs. PDAs in both phases correspond to type II in Toyozawa's classification[36] and it is consistent with a very low quantum efficiency of fluorescence. Su has calculated the stabilization energy of triplet exciton polaron (triplet STE) in PDA as 0.46 eV.[52]

2.4. Femtosecond time-resolved resonance Raman gain spectroscopy in PDA-3BCMU

Time-resolved resonance Raman spectroscopy has been recognized as a powerful method for studying structures of transient species and electronic excited states. Terai et al. have calculated phonon modes of localized excited states in PA and predicted that solitons and polarons can be distinguished by Raman spectroscopy.[53] However, only a few time-resolved Raman experiments have been done in conjugated polymers[54-57] because of the difficulties due to very short lifetime (about 1 ps) and near-infrared absorption of the excited states. Zheng et al. have investigated picosecond transient Raman scattering in PDA-4BCMU (4-butoxycarbonylmethylurethane) and observed the reduction of the Raman intensity due to the saturation of the Raman cross-section caused by photogenerated excitons.[54] Lanzani et al. have measured transient photoinduced resonance Raman scattering in PA using two color picosecond dye lasers.[55] However, since the laser pulses are resonant with the absorption from the ground state, the observed signal $\Delta I/I$ is negative and has been explained using the phase space filling model. To the best of our knowledge new phonon modes of excited states in conjugated polymers have not been observed by the transient resonance Raman spectroscopy, because two color ultrashort pulses which are resonant with the absorption from the ground state and from the excited state, respectively, and a near-infrared detector with high sensitivity are needed for the experiment. In this section, the configuration of main chain in a polydiacetylene PDA-3BCMU (3-butoxycarbonylmethylurethane) has been investigated by femtosecond time-resolved resonance Raman gain spectroscopy.

In the experiment the amplified pulse was split into three beams. The first beam (pump-1) was resonant with the excitonic absorption and generated excited states in PDA. The second one was focused in a 3-mm cell containing CCl_4 and femtosecond white continuum was generated by self-phase modulation (SPM). A part of the white continuum was selected with a set of prism pairs and a slit and amplified by a two-stage dye amplifier pumped by the second-harmonic of the Q-switched Nd:YAG laser. An interference filter (CORION, S10-700-F) was inset between the amplification stage to suppress the amplified spontaneous emission and to stabilize the wavelength. The amplified pulse has the center photon energy of 1.78 eV and the duration of 200 fs. The 1.78-eV pulse (pump-2) was resonant with the absorption from the STE and was used for the pump pulse of the Raman gain spectroscopy. The probe pulse was white continuum generated from the last beam by SPM and detected with a polychromator/CCD system. Using this technique the time dependence and spectra of photoinduced absorption, bleaching, stimulated emission, and Raman gain were observed at the same time. The Raman gain signal was distinguished using the time dependence and sharp structure, because the photoinduced absorbance change and luminescence in PDA have finite lifetime longer than 150 fs and broad spectra.[35,41,43,58,59] Polarizations of the three beams were parallel to oriented polymer chains of PDA-3BCMU deposited on a KCl crystal.[2] All the experiment was done at room temperature.

Figure 2.4.1 shows transient absorption spectra induced by the 1.97-eV pulse (pump-1), which is exactly resonant with an excitonic absorption peak. When the pump and probe pulses overlap in time at the sample, three sharp negative peaks are observed. The peak at 1.97 eV is due to saturation of the excitonic absorption and coherent coupling between pump polarization and probe field.[58] The other two peaks at 1.79 and 1.71 eV are due to the Raman gain of the stretching vibration modes of C=C and C≡C bonds, respectively. The photoinduced absorbance change below 1.8 eV shifts to higher energy with time from 0.0 to 0.5 ps. This spectral change has been explained by the relaxation model shown in Fig.2.4. 2 .[35,41,58] The FE (state 1) photoexcited by the pump-1 pulse is coupled with the stretching modes of carbon atoms within the phonon periods of 10-20 fs and becomes nonthermal STE (state 2). Then the nonthermal STE relaxes to the bottom of the potential surfaces (quasithermal STE, state 3) by quasithermalization process. Therefore, the transient absorption is shifted to higher energy and the transient fluorescence of the FE decays very rapidly as observed by PSS.[59] The STE relaxes to the ground state (G) by tunneling in the configuration space before thermalization with the time constant of 1.5 ps. The 1.78-eV pulse (pump-2) is resonant with the transition observed at 1.8 eV. This absorption peak is assigned to the transition from the STE to a biexciton with ^1A_g symmetry.[35,58]
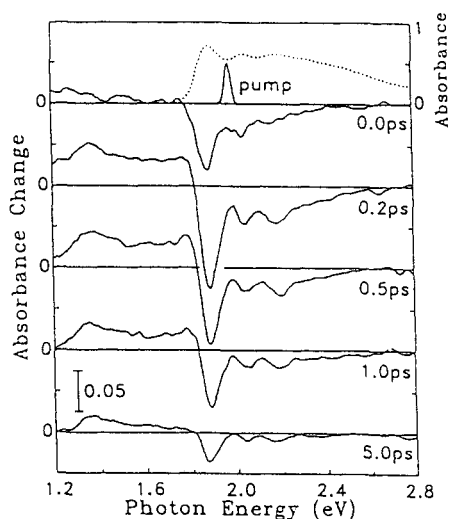

Fig. 2.4.1. Transient absorption spectra induced by the 1.97-eV pulse in PDA-3BCMU. The stationary absorption spectrum and the spectra of the 1.97-eV (pump-1) and 1.78-eV (pump-2) pulses are shown together. The excitation photon density is 1.7×10^{15} photons/cm^2.
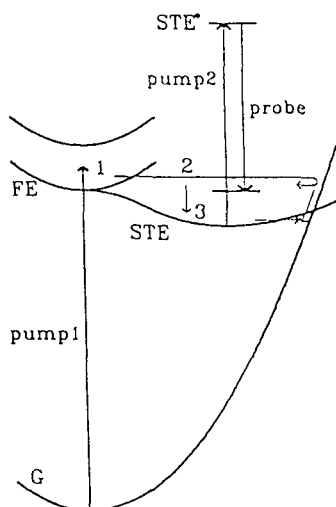

Fig. 2.4.2. Relaxation model in polydiacetylene shown in potential surfaces of excitons. States 1, 2, 3, and G are free exciton (FE), nonthermal self-trapped exciton (STE), quasithermal STE, and the ground state, respectively. STE* is a biexciton state with ^1A_g symmetry.

Transient absorption spectrum induced by the 1.78-eV pulse (pump-2) is shown in Fig.2.4.3. The pump-2 and probe pulses pass through the sample simultaneously. Two minima due to the Raman gain are clearly observed at 1.60 and 1.52 eV. The broad positive absorbance change is due to the photogenerated excitons, because the 1.78-eV pulse excites the edge of the excitonic absorption. The Raman gain spectra is obtained by subtracting the absorption spectra due to the excitons from the observed absorbance change. The absorption spectra of the excitons are estimated from the data in the regions at 1.42-1.46 eV and 1.67-1.71 eV using a quadratic equation, because the spectra have no sharp structure between 1.4 and 1.8 eV except the Raman gain signals as shown in Fig.2.4.1.
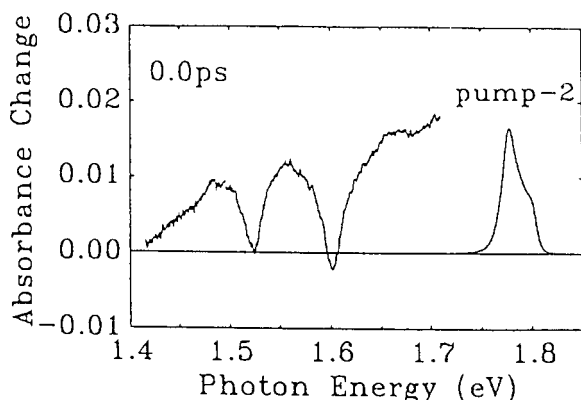
Fig. 2.4.3. Transient absorption spectrum of PDA-3BCMU induced by the 1.78-eV pulse (pump-2). The excitation photon density is 9.0×10^{15} photons/cm^2.

Figure 2.4.4(a) shows the normalized Raman gain spectra obtained using the 1.78-eV pulse at several delay times after the 1.97-eV photoexcitation. At -0.5 ps, two Raman gain peaks are observed at 1440 and 2060 cm^{-1}. They are assigned to the stretching vibrations of the C=C and C≡C bonds in the acetylene-like structure of the ground state. The spectrum at 0.0 ps has broad signal below the 1440 cm^{-1} Raman peak down to 1000 cm^{-1}. At delay time longer than 0.2 ps the Raman signal has a clear peak at 1200 cm^{-1}. The spectral change of the Raman signal around 1200 cm^{-1} is reproducible and is observed also in PDA-C$_4$UC$_4$. The width of the 2060 cm^{-1} Raman signal becomes slightly broader after the photoexcitation, but no new Raman peak is observed around 2000 cm^{-1}.

Figure 2.4.4(b) shows the transient Raman gain change at 1200 and 1440 cm^{-1}. The negative change at 1440 cm^{-1} is explained by the depletion of the ground state due to the formation of STE. The time dependence is consistent with the decay kinetics of the STE. The signal appears slightly slower than the 1.97-eV pump pulse and decays within several picoseconds. The solid curve is the best fitted curve using the formation time constant of 150 fs and 1.5 ps. The change at 2060 cm^{-1} is also negative and has similar time dependence with the 1440-cm^{-1} signal. The time dependence of the Raman signal at 1200 cm^{-1} has two components. The long-life component decays within several picoseconds and is assigned to the STE. The short-life component has time constant shorter than the present resolution time of 300 fs and is probably due to the nonthermal STE, because the 1.78-eV pulse can be resonant with the transition between the nonthermal STE and the ground state.
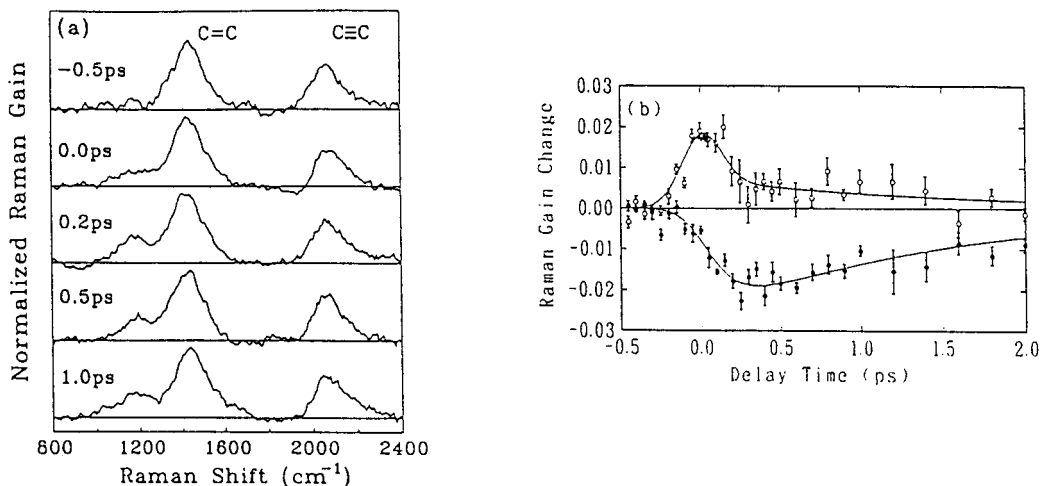

Fig. 2.4.4. (a) Normalized resonance Raman gain spectra at several delay times and (b) transient Raman gain changes at 1200 cm^{-1} (open circles) and 1440 cm^{-1} (closed circles) of PDA-3BCMU after the 1.97-eV photoexcitation. The solid curves in (b) are the best fitted curves with time constants of 150 fs and 1.5 ps. The resolution time is 300 fs. The excitation photon densities of the 1.97-eV and 1.78-eV pulses are 2.9×10^{15} and 9.0×10^{15} photons/cm^2, respectively.

The Raman signal of the ground state in PDA has a weak peak assigned to the bending mode of the C=C bond around 1200 cm^{-1}.[60,61] Therefore, the observed 1200 cm^{-1} Raman signal may be explained by the increase in the Raman cross-section of the bending mode. However, since the 1200 cm^{-1} spectrum at 0.0 ps is broader than at later times, this spectral change cannot be explained by the increase of the cross-section. It suggests that the geometrical

relaxation of main chain configuration due to the self-trapping process takes place after the 1.97-eV photoexcitation. Since the wave packet of the nonthermal STE oscillates in the configuration space as shown in Fig.2.4.2, the Raman signal due to the nonthermal STE is broad. After the quasithermalization, the nonthermal STE relaxes to the bottom of the STE potential surface. Therefore, the oscillatory motion in the configuration space becomes smaller and the clear Raman peak is observed at 1200 cm^{-1}.

The theoretical calculation has predicted that the localized excitations in *trans*-PA have several Raman active phonon modes.[53] The expected signal is the reduction of the stretching vibration modes and new Raman lines at lower frequencies than the stretching modes. The Raman signal observed in PDA is similar to this feature. However, the phonon modes of the STE in PDA have not been investigated. Here, the observed Raman frequency is compared with stretching modes of center bonds in unsaturated hydrocarbons with four carbon atoms, i.e. repeat units of PDA.[62] The formation of the STE in PDA is expected to be the geometrical relaxation from the acetylene-like structure (=CR-C≡C-CR=)$_x$ to the butatriene-like structure (-CR=C=C=CR-)$_x$. The C=C bond in *trans*-butene-2 (CH$_3$-CH=CH-CH$_3$) has a stretching mode with 1675 cm^{-1}, while the frequency of the C-C bond in *trans*-1,3-butadiene (CH$_2$=CH-CH=CH$_2$) is 1202 cm^{-1}. Therefore, the 1200 cm^{-1} Raman peak can be assigned to the C-C bond in the butatriene-like structure. However, Raman signal due to the C=C bond in the butatriene-like structure cannot be observed in this study. It may be explained by close frequencies of the stretching modes of the center C=C bond in butatriene (CH$_2$=C=C=CH$_2$) and the C≡C bond in dimetylacetylene (CH$_3$-C≡C-CH$_3$), 2079 and 2235 cm^{-1}, respectively. The expected new Raman signal near the 2060 cm^{-1} peak is not resolved in this study because of the broad pump spectrum.

The intensity of the 1200 cm^{-1} peak is about one third of that of the 1440 cm^{-1} peak as shown in Fig.2.4.4(a) and the change at 1200 cm^{-1} is also smaller than the change at 1440 cm^{-1}. The resonance Raman signal of the ground state pumped by the 1.78-eV pulse is estimated to be about 15% of that pumped by the 1.97-eV pulse using the homogeneous and inhomogeneous widths of the excitonic absorption of the PDA-3BCMU.[41] The absorbance of the sample at 1.97 eV is 0.8, while the maximum transient absorbance at 1.78 eV is 0.13 when the STE is generated by the 1.97-eV pulse with the density of 2.9x10^{15} photons/cm^2. Therefore, if the ground state and STE have the same Raman cross-section, the Raman signals due to the STE and the ground state are estimated to have almost the same intensity. The smaller 1200 cm^{-1} signal indicates that the Raman cross-section of the STE is smaller than that in the ground state. It is mainly due to broader absorption spectrum of the transition from the STE to higher excited states than the excitonic absorption from the ground state.

3. CONCLUSION

The exciton energy dependence of the ultrafast relaxation processes has been investigated in the PDA-(12,8) LB films with three exciton transition energies. The relaxation of exciton is faster in PDA with lower exciton energy. The decay kinetics is discussed using the model potential curves of FE, STE, and the ground state. The main relaxation mechanism from STE to the ground state is the tunneling in the configuration space. The dependencies of the decay kinetics on the exciton energy and temperature are well explained. The stabilization energy of STE and the barrier height between STE and the ground state are estimated.

The new Raman peak due to photoexcited states in PDA has been observed at 1200 cm^{-1} for the first time by the femtosecond time-resolved Raman gain spectroscopy. The observed Raman signals indicate that the acetylene-like structure of the main chain relaxes to the butatriene-like structure due to the formation of the self-trapped exciton with the geometrical relaxation. The formation and decay kinetics of the Raman signals is consistent with the relaxation processes of excitons observed by femtosecond absorption and fluorescence spectroscopies.

Some discussions presented here have already appeared elsewhere [63] and cited in the text.

4. ACKNOWLEDGMENTS

5. REFERENCES

1. T. Kobayashi, ed., *Nonlinear Optics of Organics and Semiconductors*, Springer-Verlag (Berlin) (1989).

2. M. Sinclair, D. Moses, K. Akagi, and A.J. Heeger, Phys. Rev. B38 **38**, 10724-10733 (1988).

3. W.S. Fann, S. Benson, J.M.J. Madey, S. Etemad, G.L. Baker, and F. Kajzar, Phys. Rev. Lett. **62**, 1492-1495 (1989).

4. W.P. Su and J.R. Schrieffer, Proc. Natl. Acad. Sci. **77**, 5626-5629 (1980).

5. C.V. Shank, R. Yen, R.L. Fork, J. Orenstein, and G.L. Baker, Phys. Rev. Lett. **49**, 1660-1663 (1982).

6. L. Rothberg, T.M. Jedju, S. Etemad, and G.L. Baker, IEEE J. Quantum Electron. **QE-24**, 311-314 (1988).

7. A.J. Heeger, S. Kivelson, J.R. Schrieffer, and W.P. Su, Rev. Mod. Phys. **60**, 781-850 (1988).

8. M. Yoshizawa, T. Kobayashi, H. Fujimoto, and J. Tanaka, J. Phys. Soc. Japan **56**, 768-780 (1987).

9. M. Yoshizawa, T. Kobayashi, H. Fujimoto, and J. Tanaka, Phys. Rev. B **37**, 8988 (1988).

10. M. Yoshizawa, T. Kobayashi, K. Akagi, and H. Shirakawa, Phys. Rev. B **37**, 10301-10307 (1988).

11. P.D. Townsend and R.L. Friend, Phys. Rev. B 40, 3112-3120 (1989).

12. G. Wegner, Makromol. Chem. 145, 85-94 (1971).

13. G. Wegner, Makromol. Chem. 154, 35-48 (1972).

14. R.H. Baughman and K.C. Yee, J. Polym Sci., Macromol. Rev. 13, 219-239 (1978).

15. R.H. Baughman, J. Polm. Sci., Polym. Ed. 12, 1511-1535 (1974).

16. D. Bloor, *Polydiacetylenes,* D. Bloor and R.R. Chance ed., Martinus Nijhoff Publishers (Dordrecht, Netherlands) (1985) .

17. D. Bloor, S.D.D.V. Rughooputh, D. Phillips, W. Hayes, and K.S. Wong, in *Electronic Properties of Polymers and Related Compounds,*
    H. Kuzmany, M. Mehring, and S.Roth. ed. (Springer-Verlag (Berlin), 1985) .

18. K.C. Lim, A. Kapitunik, R. Zacher, and A.J. Heeger, J. Chem. Phys. 82, 516-521 (1985).

19. K.C. Lim and A.J. Heeger, J. Chem. Phys. 82, 522-530 (1985).

20. R.R. Chance, G. Patel, and J.D. Witt, J. Chem. Phys. 71, 206-211 (1979).

21. G.N. Patel, R.R. Chance, and J.D. Witt, J. Chem. Phys. 70, 4387-4392 (1979).

22. T. Kanetake, Y. Tokura, T. Koda, T. Kotaka, and H. Ohnuma, J. Phys. Soc. Japan 54, 4014-4026 (1985).

23. T. Kobayashi, K. Ogasawara, S. Koshihara, K. Ichimura, and R. Hara, in *Primary Processes in Photobiology,* T. Kobayashi ed.
    (Springer-Verlag, Berlin Heidelberg, 1987) pp.125.

24. B.I. Greene, J. Orenstein, R.R. Millard, and L.R. Williams, Chem. Phys. Lett. 139, 381-385 (1987).

25. G.M. Carter, J.V. Hryniewicz, M.K. Thakur, Y.J. Chen, and S.E. Meyler, Appl. Phys. Lett. 49, 998-1000 (1986).

26. T. Kobayashi, J. Iwai, and M. Yoshizawa, Chem. Phys. Lett. 112, 360-364 (1984).

27. T. Kobayashi, M. Yoshizawa, U. Stamm, M. Taiji, and M. Hasegawa, J. Opt. Soc. Am. B 7, 1558 (1990).

28. M. Yoshizawa, M. Taiji, and T. Kobayashi, IEEE J. Quantum Electron. QE-25, 2532-2539 (1989).

29. U. Stamm, M. Taiji, M. Yoshizawa, T. Kobayashi, and K. Yoshino, Mol. Cryst. Liq. Cryst. 182A, 147-156 (1990).

30. J. Jortner, in *Excitons ,* E.I. Rashba and M.D. Sturge ed. (North-Holland, Amsterdam , 1987) .

31. C.X. Cui and M. Kertesz, Phys. Rev. B40, 9661 (1989).

32. G. Gustafson, O. Inganas, H. Osterholm, and J. Laakso, in press.

33. K. Nasu, J. Luminescence 38, 90-92 (1987).

34. H. Sumi, M. Georgier, and A. Sumi, Rev. Solid State Sci. 4, 209 (1990).

35. T. Kobayashi, Nonlinear Optics 2, 101 (1992).

36. Y. Toyozawa, J. Phys. Soc. Japan 58, 2626 (1989).

37. Y. Toyozawa, Electron induced lattice instabilities, unpublished.

38. D. McBranch, A. Heys, M. Sinclair, D. Moses, and A.J. Heeger, Phys. Rev. B 42, 3011 (1990).

39. R.H. Friend, D.D.C. Bradley, and P.D. Townsend, J. Phys. D20, 1367 (1987).

40. J.H. Burroughes, D.D.C. Bradley, A.R. Brown, R.N. Marks, K. Mackay, R.H. Friend, P.L. Burns, and A.B. Holmes, Nature 347, 538
    (1990).

41. M. Yoshizawa, A. Yasuda, and T. Kobayashi, Appl. Phys. B 53, 296 (1991).

42. M. Movaghar, G.W. Sauger, D. Wurtz, and D.L. Huber, Solid State Comm. 39, 1179-1182 (1981).

43. M. Yoshizawa, K. Nishiyama, M. Fujihira, and T. Kobayashi, Chem. Phys. Lett., 207, 461(1993).

44. D. Birnbaum, B.E. Kohler, and C.W. Spangler, J. Chem. Phys. 94, 1684 (1991).

45. G.W. Hayden and E.J. Mele, Phys. Rev. B34, 5484 (1986).

46. K. Ichimura, M. Yoshizawa, H. Matsuda, S. Okada, M. Osugi, S. Hourai, H. Nakanishi, and T. Kobayashi, J. Chem. Phys. 99,
    7404(1993).

47. P.L.Danielsen and R.C. Ball, J. Physique 46, 1611 (1985).

48. E. Gutsce, Phys. Stat. Sol. b 109, 583 (1982).

49. K.S. Song and C.H. Leung, Solid State Commun. 32, 565 (1979).

50. T.H. Keil, Phys. Rev. 140A, 601 (1965).

51. S. Koshihara, T. Kobayashi, H. Uchiki, T. Kotaka, and H. Ohnuma, Chem. Phys. Lett. 114, 446-450 (1985).

52. W.P. Su, Phys. Rev. B36, 6040 (1987).

53. A. Terai, Y. Ono, and Y. Wada, J. Phys. Soc. Jpn. 58, 3798 (1989).

54. L.X. Zheng, R.E. Benner, Z.V. Vardeny, and G.L. Baker, Synth. Metals 49, 313 (1992).

55. G. Lanzani, L.X. Zheng, G. Figari, R.E. Benner, and Z.V. Vardeny, Phys. Rev. Lett. 68, 3104 (1992).

56. G. Lanzani, L.X. Zheng, R.E. Benner, and Z.V. Vardeny, Synth. Metals 49, 321 (1992).

57. D.L. Weidman and D.B. Fitchen, Proc. 10th Int. Conf. Raman Spectroscopy Univ. of Oregon, Eugene , 12 (1986).

58. M. Yoshizawa, Y. Hattori, and T. Kobayashi, Phys. Rev. B 47, 3882 (1993).

59. A. Yasuda, M. Yoshizawa, and T. Kobayashi, Chem. Phys. Lett. 209, 281 (1993).

60. D.N. Batchelder and D. Bloor, J. Phys. C C15, 3005 (1982).

61. W.F. Lewis and D.N. Batchelder, Chem. Phys. Lett. 60, 232 (1979).

62. L.M. Sverdlov, M.A. Kovner, and E.P. Krainov, in *Vibrational Spectra of Polyatomic Molecules* (John Wiley & Sons, New York,
    Toronto, 1970) pp.282.

63. M. Yoshizawa, Y. Hattori, and T. Kobayashi, Phys. Rev. B49, 13259 (1994).